Limit Analysis of RC Slabs
with
Equilibrium Finite Elements

Complementary Technology

$$\overbrace{\lambda_{EFE} \leq \lambda \leq \lambda_{SLAB}}^{\text{Verification – Simulation Governance}}$$

Statically Admissible
Moment Field
Hillerborg - Design

Kinematically Admissible
Collapse Mechanism
Johansen - Assessment

EFE – How it Works

Load Factor　　　Variables

$$m = \lambda_{EFE} m_0 + \phi m_h$$

Particular Moments　　　Hyperstatic Moments

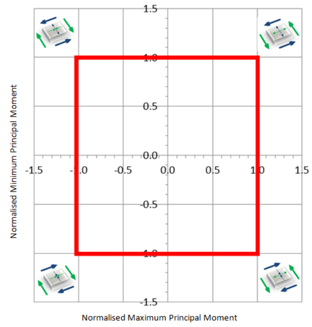

Strength Criterion

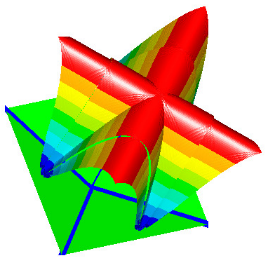

Total Solution (λ =24 - exact)

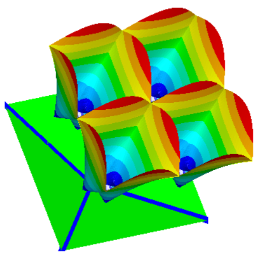

Particular Solution (λ =13.8)

Making the Most of Your Structure

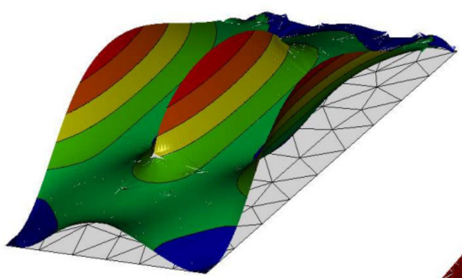

Elastic

Plastic

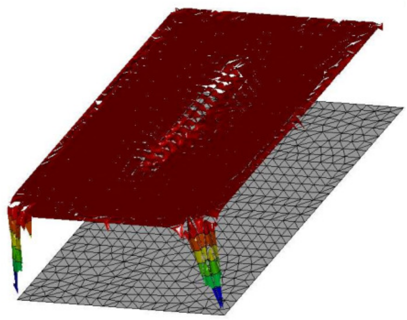

Limit load 2.7 times load to cause first yield

Of course you will get more if you consider strain hardening and membrane action…

Flat Slab on Regular Array of Columns

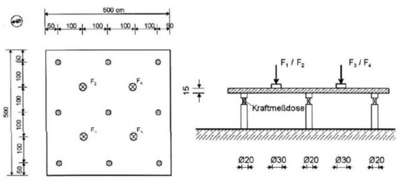

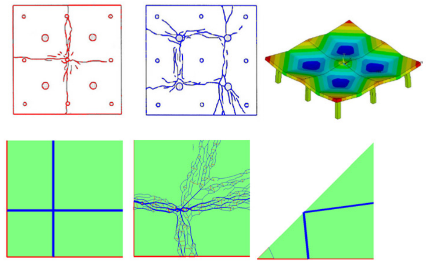

(a) Quarter (Structured) (b) Quarter (Unstructured) (c) Eighth (Optimised)

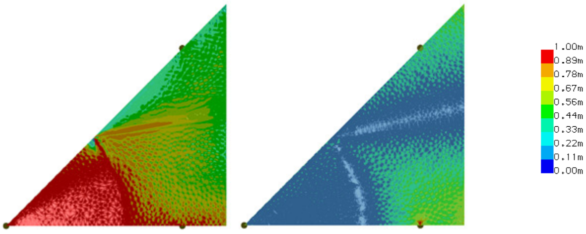

Irregular Flat Slab on Blade Columns

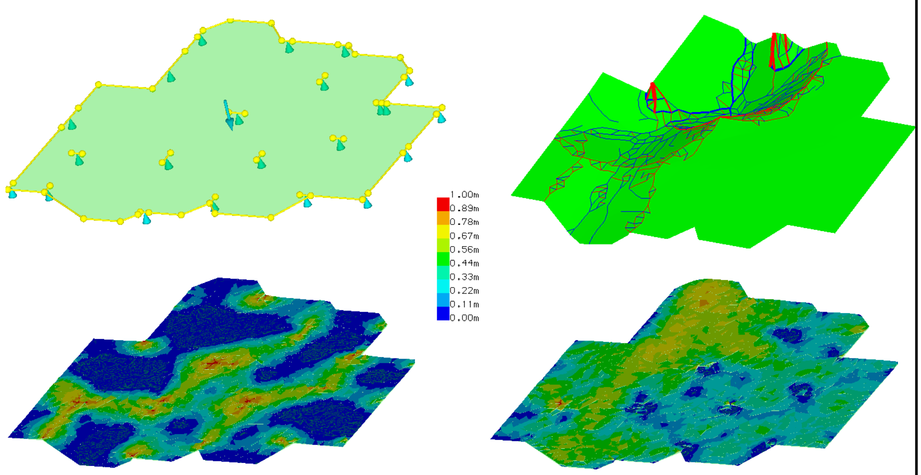

EFE as a Plugin to SLAB

Initial EFE plugin to use SLAB's yield lines to delineate an initial mesh for EFE and we are confident of obtaining very close bounds to the collapse load (1% in 1 Second).

A future EFE plugin could include:

- Metallic plates,
- Elastic analysis,
- Transverse shear force fields,
- Design optimisation based on design variables as well as statical variables,
- Shakedown,
- Limited ductility in RC slabs,
- Membrane actions and the effects of large deflections.

EFE - Admissible with Design Codes!

The **fib Model Code for Concrete Structures 2010** allows the use of the theory of plasticity in design, and this includes the "**lower bound (static) theorem**" (clause 7.2.2.4.3). However the Code appears to keep very quiet concerning the mechanics of using this theorem!

Verification of designs may be assisted by numerical simulations, including the finite element method (clause 7.11.2.2). This clause warns that "In the case of the most widely used stiffness method, the shape of the displacement field is assumed and **equilibrium is satisfied only in integral sense**. **The internal stresses are lower, compared with an exact solution**. **The approximations introduced by the finite element formulation only, can be a significant source of errors in numerical analysis**".

NB: in the lower bound plug-in, the finite element method that is used assumes fields of stresses, instead of displacements, which satisfy equilibrium exactly. Hence a source of error found in the conventional finite element method is removed.

Stress Resultant Trajectories

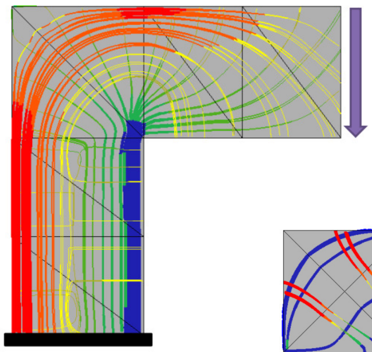

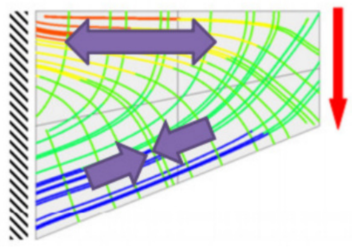

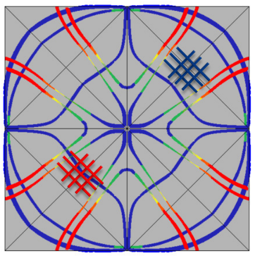

Thank you for listening!

Letter to Verulam – Effective Width of Slabs

Original Letter

Ramsay Maunder Associates,

Institution of Structural Engineers,
International HQ,
11 Upper Belgrave Street,
London SW1X 8BH.

9th November 2010

Dear Editor of Verulam,

We would like to add to the discussion initiated by John Botterill (Verulam, 5th May 2010) on the width of slab to be considered to carry a concentrated load ("shear loads on slabs"), and the replies by Bill Wadsworth and Charles Goodchild (Verulam, 19th October 2010). The question of effective width raises interesting questions relating to the use of EC2, the use of elastic and limit analyses, and ductility.

EC2 is written as a general rather than a prescriptive code of practice, thus relying on the engineer to carry out appropriate structural analyses, or refer to standard solutions if they exist, rather than provide guidance rules for the concentrated load problem.

Referring to the elastic analysis of the problem as defined by Bill Wadsworth, it would seem to us that finite element models can be used to provide reliably accurate distributions of moment and shear throughout the slab. We considered the case of a central concentrated load, and found that the distributions converged to values a little different from Bill's finite difference method based on a horizontal grid spacing of 0.75m parallel to the supports – Figures 1 and 2. We have confidence in our results since we have good agreement between both conforming and equilibrating finite element models (referred to as EFE in figures 1 and 2). We have assumed the load to be uniformly distributed over a square area of side length 0.2m which is also taken as the thickness of the slab. So the main difference in the moments occurs under the load, which might be expected, but a bigger difference occurs for the shear force at the centre of a support, and the finite element models recognise the concentrated downward reactions located at the ends of the supports.

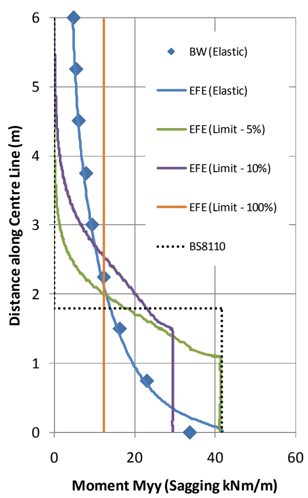

Figure 1: Bending Moments at Midspan

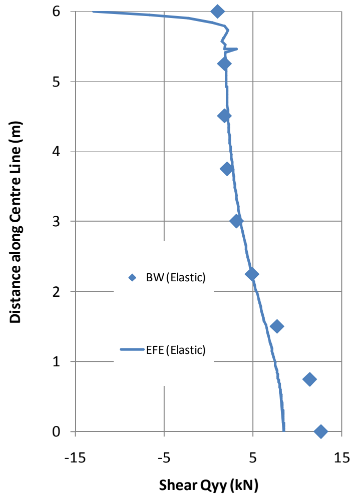

Figure 2: Reactions

So what moments and forces should be used in design, particularly if we want to justify designing for smaller moments in the neighbourhood of the load? EC2 allows us to exploit plastic methods and use limit analyses, although it doesn't appear to be prescriptive as regards ductility in this situation! We have carried out limit analyses based on the yield line method for upper bounds, and a method for lower bounds based on equilibrium finite element models (EFE), for various arrangements of orthotropic reinforcement (assuming equal top and bottom reinforcement for simplicity). Results from the yield line method indicate that a single circular fan mechanism is not the most critical mechanism, but rather some variation on the mechanism in Figure 3. The interesting feature of the lower bound results plotted in Figure 4 is that the region of slab that is fully utilised by yielding tends to form a well defined band for highly orthotropic reinforcement, and the width of this band agrees well with the dimensions of the corresponding yield line pattern. This gives us confidence in the limit solutions which agree as regards the limit load to within 10%. The results in figure 1 for bending moments across the 12m width of slab in Bill's example indicate the extent of moment redistribution from the elastic state.

So from the design point of view the limit analyses provide a rational way to redistribute moments throughout the slab, and this leads to much lower moments in the neighbourhood of the load. Can we safely base ULS design on these moments? This raises the question of ductility, as would a design based on a simple fan mechanism if this was appropriate, since with equal top and bottom reinforcement in the isotropic case this mechanism would imply the need for moment capacities of only some 8kNm/m (P/4π), instead of some 40kNm/m from the elastic analyses!! It would appear from Section 5.6 Plastic analysis in EC2 that rotation capacity needs to be checked, but do the same rules apply for slabs as in the current problem as for continuous beams? If so, how then is the value of a moment to be defined when we recognise that moment becomes a tensor quantity rather than a scalar?

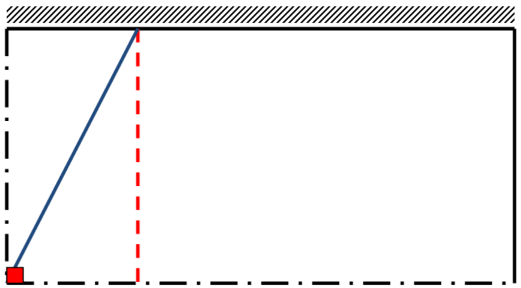

Figure 3: Yield-Line Pattern

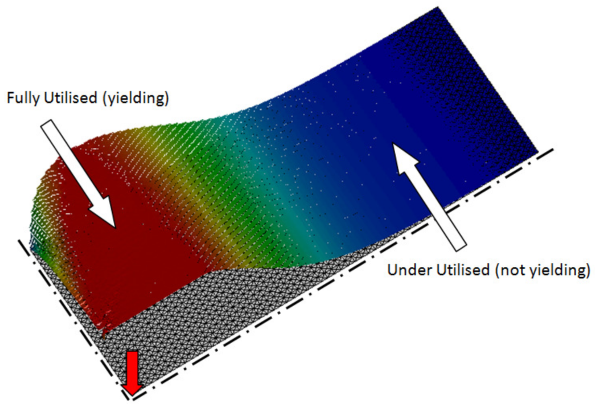

Figure 4: Contours of Utilisation from EFE

Further details of the equilibrium finite element models (EFE) used in this study and more comprehensive results may be seen at www.ramsay-maunder.co.uk.

Yours sincerely,

Edward Maunder FIStructE & Angus Ramsay MIMechE.

Note on Support Conditions

In our response to the Letter to Verulam on the Effective Width of Slabs, we presented (shear) reactions (figure 2 in our letter) with the units kN. These should have been reported as distributions with the units of kN/m.

Our analysis considered the simple support conditions as being 'hard' with boundary twist restrained and non-zero torsional moment reactions. Correspondence with Bill Wadsworth revealed that in his analysis he had assumed 'soft' simple supports with free boundary twist and and zero torsional moment reactions. The different support conditions (hard versus soft) lead to different shear reactions and this explains the difference in our results and those of Bill Wadsworth. The following figure illustrates this difference using our EFE software – we have used cubic moment fields for the elastic analysis with SS representing soft-simple and HS representing hard simple support conditions.

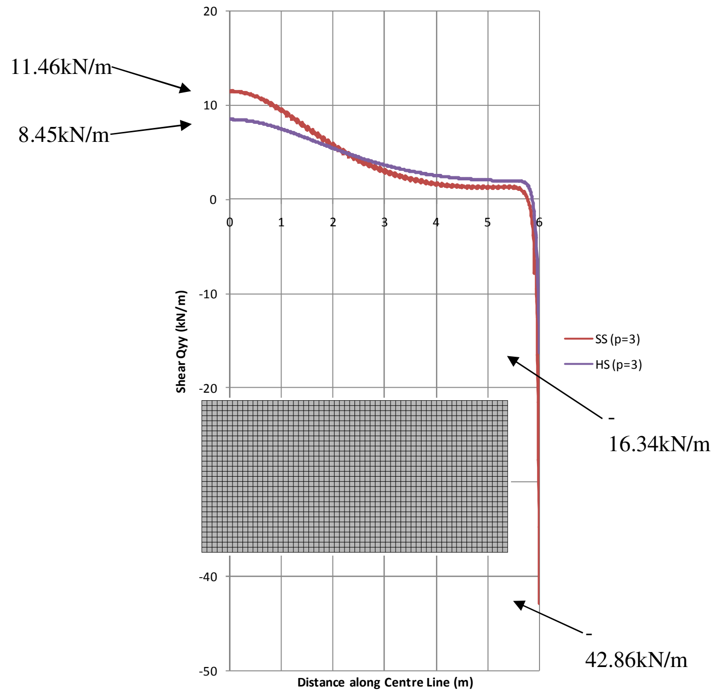

Figure 1: Reaction distributions for Verulam Problem with Hard & Soft Simple Supports

Supplement to Letter

Background

RMA has developed equilibrium finite element software (EFE) for the elastic and plastic design and assessment of, amongst others, reinforced concrete slabs and bridge decks. The ongoing Verulam discussion on Effective Width of Slabs was of interest to us since, with the safe plastic analysis techniques available within EFE, the calculation of effective widths, albeit currently assuming adequate ductility, is simply conducted. We submitted a letter to The Structural Engineer summarising the results obtained from EFE on a particular slab configuration discussed in the letter. Here we present supplementary results which, for reasons of space, did not go into the letter.

Elastic Solution

The slab configuration considered in Verulam is a 12m by 6m one-way (short dimension) spanning simply supported slab with central point load. A 6m by 3m symmetric quadrant of the slab was modelled as shown in figure 1.

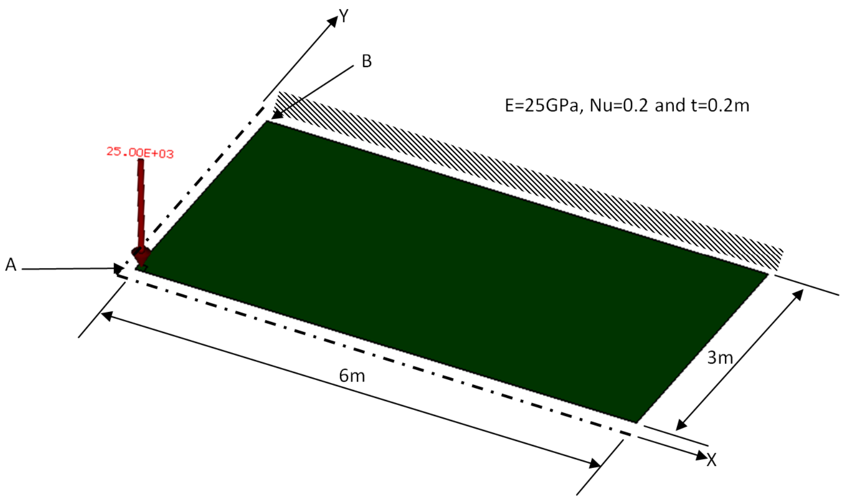

Figure 1: Geometry, material, boundary conditions and loading

The elastic properties and thickness are given in the figure together with the boundary conditions (symmetry on two edges and simple support on one edge) and the loading (25kN on one quadrant distributed evenly over a 0.1m by 0.1m region at the centre of the plate). The simple support condition that we model is 'hard', in the context of Reissner-Mindlin plate theory, i.e. torsional moments form part of the reactions.

A mesh refinement study using the two meshes shown in figure 2(a) and (b) was conducted with moment fields varying from quadratic to quartic (degree 2 to 4).

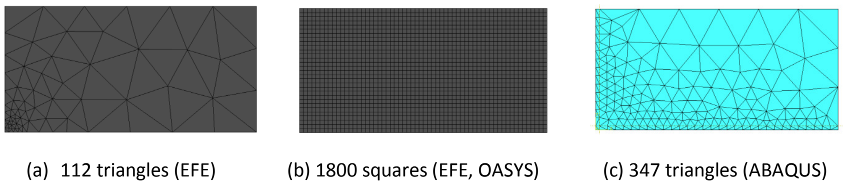

Figure 2: Finite element meshes

Three quantities of interest were monitored for convergence these being the transverse displacement at point A, the moment Myy at point A and the shear Qy at point B. The results are shown in table 1 which also includes FE results from ABAQUS and OASYS (both programs use conventional conforming elements), Bill Wadsworth's finite different results (BW) and Robert Hairsine's grillage results (RH). Note that RH's results have been inferred from his letter (Verulam, 16th November 2010) where he states that his results were within 10% and 5% of BW's results respectively for moments and shears – we have assumed that the results take him nearer to the correct value.

The mesh refinement study indicates that the results obtained for the 112 mesh with quartic moment fields have converged as they are identical to the much more refined 1800 element mesh. The conventional conforming finite element models agree well with EFE when quadratic displacement fields are used – the results for the linear displacement elements are, as expected, less accurate.

It is interesting to note how different the finite difference and grillage results are from the true values – 20% underestimate for moment and 42% overestimate for shear. It is interesting also to see how good the results from EFE are for the coarse model.

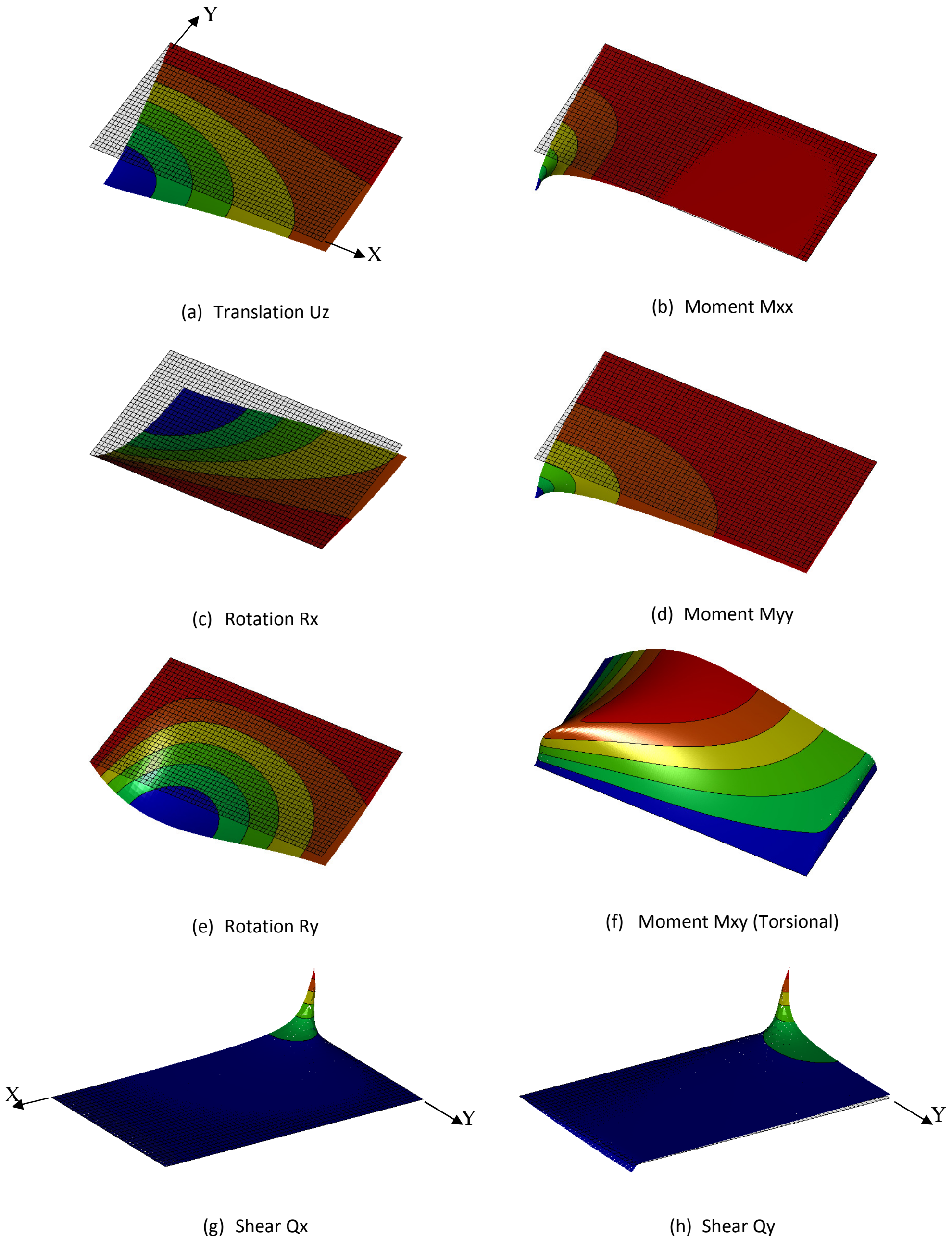

Figure 3: Contour plots of the displacements, Cartesian moments and shears

	Number of Elements	Degree of Moment (M) or Displacement (D)	Uz (mm)	Myy (kNm/m)	Qy (kN)	
EFE	112	2M	3.66	41.90	8.61	
	112	3M	3.66	41.94	8.46	
	112	4M	3.66	41.94	8.45	Converged
	1800	2M	3.66	41.94	8.45	Results
ABAQUS	347	1D	3.61	38.59		
	347	2D	3.66	43.58		
OASYS	1800	1D		39.44	8.44	
BW	Finite Difference			33.62	12.64	
RH	Grillage			36.98	12.01	

Table 1: Convergence of quantities of interest with mesh refinement

Contour plots of the displacements, Cartesian moments and shears are shown in figure 3. In the moment plots, hogging moments are positive and are plotted above the plane of the elements, sagging moments are negative and are plotted below. Note that these are unprocessed results, i.e. they are plots of the moments and shears from the finite element model. Unlike conforming finite elements these quantities are in equilibrium with the applied load and conform with the static boundary conditions – for example Mxx and Myy should be zero on the simply supported and free edges and Mxy should be zero on all except the simply supported edge where torsional moments were restrained (hard simple support).

One of the virtues of EFE is that, with equilibrium being satisfied *a-priori,* high quality results of practical engineering significance are immediately available. Figure 4 shows some of these results including trajectories, which aid understanding of the way in which the load is transmitted through a structure, and boundary distributions which illustrate how the load is transferred into adjacent structures.

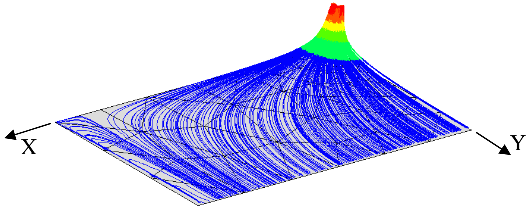

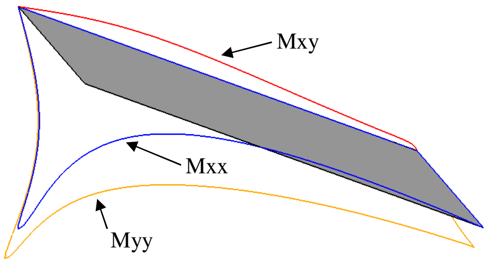

(d) Cartesian moments on model boundary

(a) Resultant shear trajectories

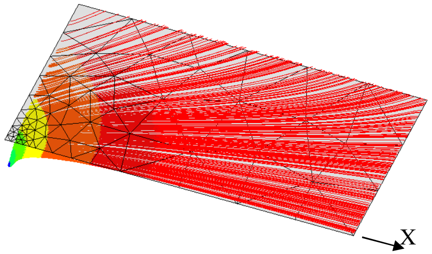

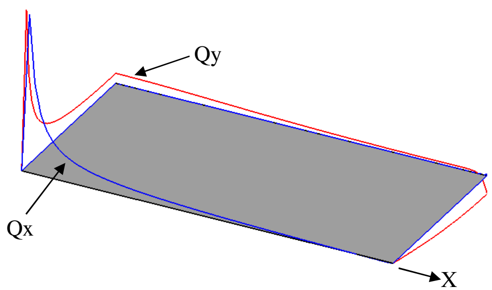

(b) Maximum principal moment trajectories

(e) Cartesian shears on model boundary

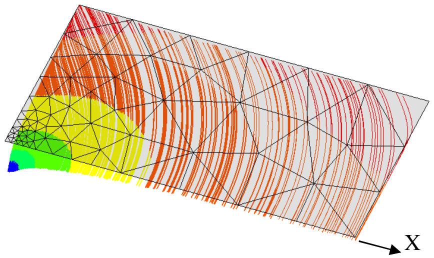

(c) Minimum principal moment trajectories

Figure 4: Plots of shear and moment trajectories and boundary distributions of moments and shear

Plastic Solution

In addition to elastic analyses, EFE performs plastic ULS analysis of, amongst others, reinforced concrete plates. The moment fields used are in equilibrium with the applied load and the Nielsen bi-conic yield criterion (or alternatively the Wood-Armer yield criterion) limits the values of the moments. The scheme is a rigorous lower-bound approach providing guaranteed safe, conservative, estimates of the flexural collapse load (when shear is not critical) irrespective of mesh refinement. The moment fields are constructed for the plastic solution based on Kirchhoff type elements which enforce continuity of bending moments and equivalent Kirchhoff shear forces.

The software also includes a conventional yield-line solver for obtaining traditional upper-bound solutions for comparison purposes. We have conducted yield line analyses for cases with yield moments of 100kNm/m for both hogging and sagging in the span direction, and with transverse yield moments at 100% (isotropic), 50%, 10% and 5% of this value. For the isotropic case, upper and lower bound solutions agree at a load factor (λ) of 8.14, and as the transverse yield moment is reduced so is the load carrying capacity. Figure 5 shows contours of utilisation for the four transverse yield moments considered.

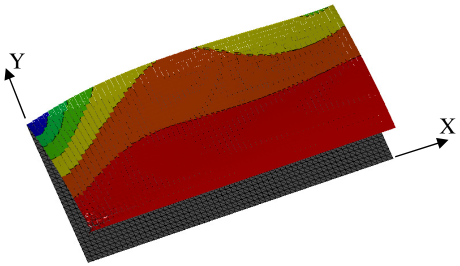

(a) 100% (λ = 8.14)

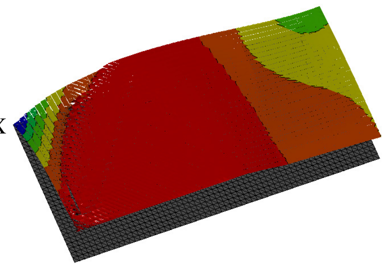

(b) 50%

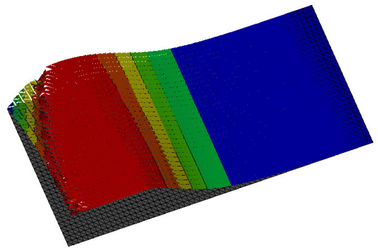

(c) 10% (λ = 3.37)

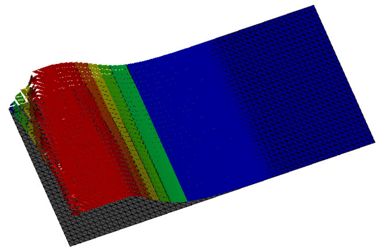

(d) 5%

Figure 5: Utilitisation for various percentages of transverse yield moment (EFE)

Figure 6 shows the yield line collapse mechanism with a single geometric variable X. In this figure the blue line represents a sagging yield line and the dashed red line a hogging yield line. This mechanism is a simplified first approximation of the true collapse mechanism which in practice will probably be more complicated. The load factor from the refined EFE model is probably within a few percent of the true value and the inset to figure 6 shows how both upper and lower bound load factors vary with the geometric variable X for the eight element mesh. It is seen that whereas the yield line solution is extremely sensitive to the value of X, the lower bound solution from EFE remains sensibly invariant despite an extremely coarse mesh.

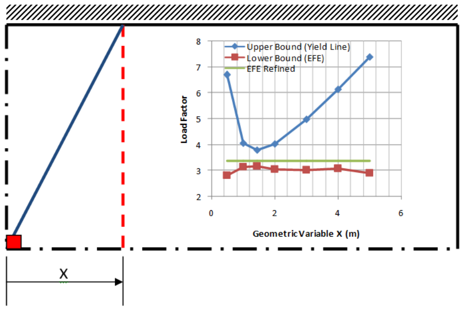

Figure 6: Geometric Optimisation for Yield Line (10% transverse yield moment)

Boundary distributions of moment are shown in figure 7 for the case of 10% transverse yield moment. It should be noted that in this figure the torsional moment Mxy is not exactly zero along the lines of symmetry, particularly in the neighbourhood of the load, this being a consequence of the use of Kirchhoff type elements.

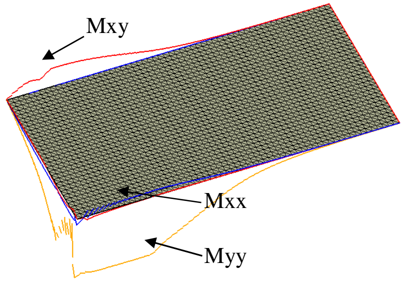

Figure 7: Boundary distributions for EFE (10% transverse yield moment)

In figure 8 the boundary distributions of bending moments along the centre line of the slab for the various analyses conducted are shown.

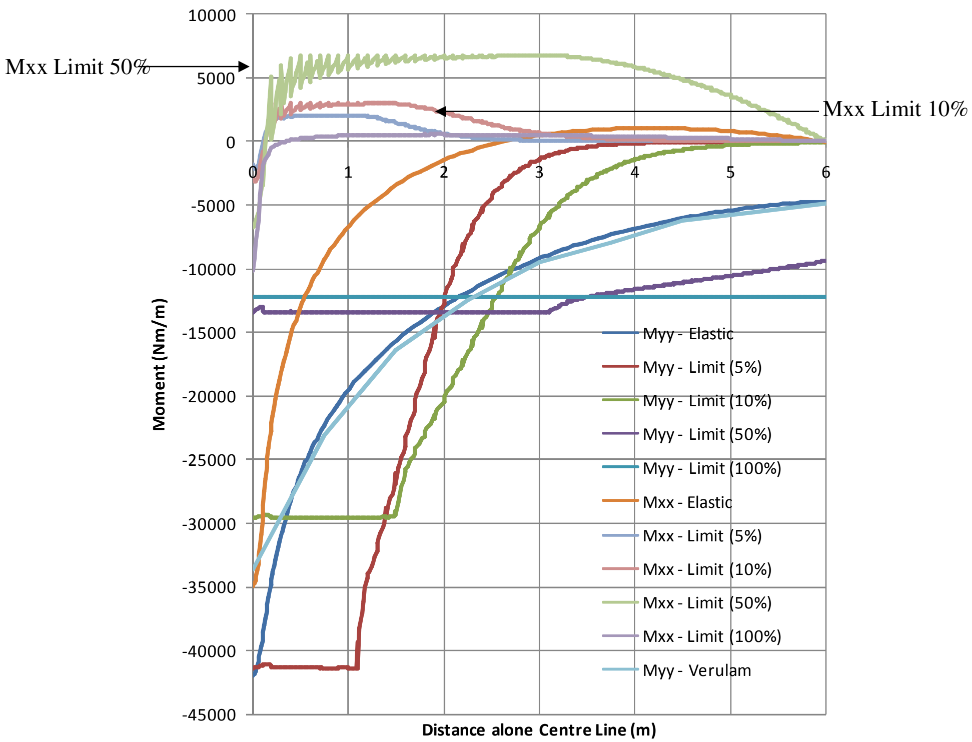

Figure 8: Distributions of Mxx and Myy along centre line (Elastic and Plastic)

Closure

We have tried to show in the original letter and now in this supplement that the application of equilibrium finite element methods (elastic and/or plastic), provide rational and safe answers to many of the questions faced by practicing structural engineers.

It is clear from this exercise that there are considerable differences between finite element results, which we believe to be close to theoretical elastic solution, and methods based on finite differences or grillage models. Finite element software is widely available and should now be an everyday tool for the practicing structural engineer.

Finite element techniques can be extended to plastic methods which, when based on equilibrium, seek lower-bound solutions. This enables the engineer to explore the potential benefits of moment redistribution. Such methods provide a rational and safe approach to answering questions such as that posed in the original Verulam letter regarding the effective width of slabs.

Ramsay Maunder ASSOCIATES *Finite Element Specialists and Engineering Consultants*

Assessment of a Pair of Reinforced Concrete Roof Slabs

Introduction

RMA have conducted analyses of a pair of reinforced concrete roof slabs for an American Precast company. RMA's finite element software EFE was used for this work. EFE conducts yield line, elastic and lower-bound limit analysis and the results from all three types of analysis applied to each slab are presented.

Geometry of Left Hand Slab

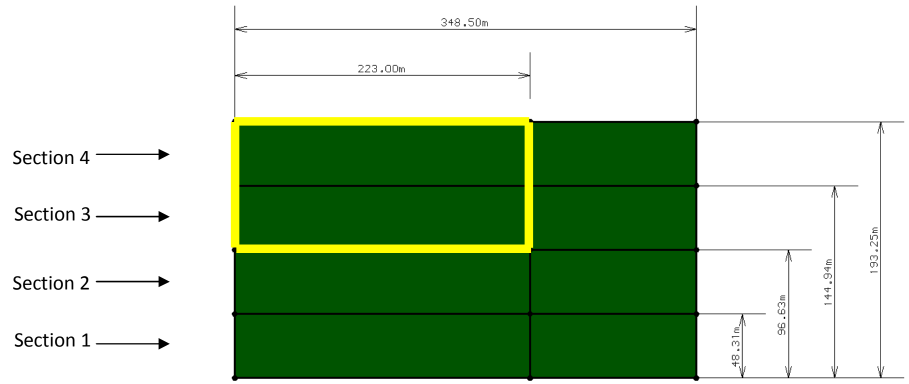

Dimensions in inches (not metres as suggested in figure)

Figure 1: Geometry and simple supports for roof slab

Properties for Left Hand Slab

The properties used for the elastic analysis were:

Elastic Modulus 3.63e6 lb/in^2 (25GPa)

Poisson's Ratio 0.2

We took account of the slab's thickness variation by breaking the slab into four sections as identified in Figure 1. The elastic analysis used the mean thickness for each section as shown in Table 1. Isotropic reinforcement was used and we assumed that the top steel had a constant cover so that the moment capacity varied linearly across the slab. In each section we used the moment capacities shown in Table 1.

Section	Thickness (in)	Moment Capacity (lb/in^2)
1	8.5	10,000
2	9.5	11,176
3	10.5	12,353
4	11.5	13,529

Table 1: Slab thicknesses and moment capacities

Loads/Boundary Conditions for Left Hand Slab

The slab was assumed to be simply supported on the four lines shown in Figure 1. The slab was loaded with uniform distributed loads corresponding to the sum of a dead load and a live load. The dead load was based on an assumed density of concrete/steel composite over the given section thickness whilst the live load was taken as a constant for the entire slab:

Dead load – density of concrete/steel composite 0.09lb/in^3 (2500kg/m^3)

Live load - 0.11lb/in^2 (0.75kN/m^2)

Table 2 lists the total loads (dead plus live) for each section.

Section	Total Load (lb/in^2)
1	0.874
2	0.964
3	1.054
4	1.144

Table 2: Slab uniformly distributed loads

Elastic Analysis Results for Left Hand Slab

A mesh of 720 square elements was used for the analyses. The elastic analysis used quadratic moment fields and the displaced shape is shown in Figure 2.

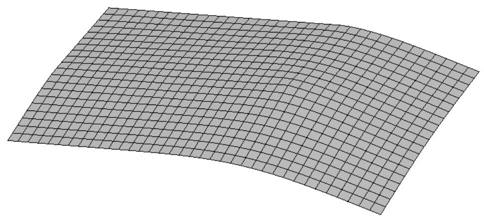

Figure 2: Displaced shape (elastic)

For the assumed elastic properties maximum displacement was -0.38in and occurred at the bottom right hand corner – as expected. A contour plot of displacement is shown in Figure 3. The contours are displaced away from the base plane mesh to aid understanding. It is seen that the slab deflects upwards inside the constrained region and the maximum positive displacement is 0.01in.

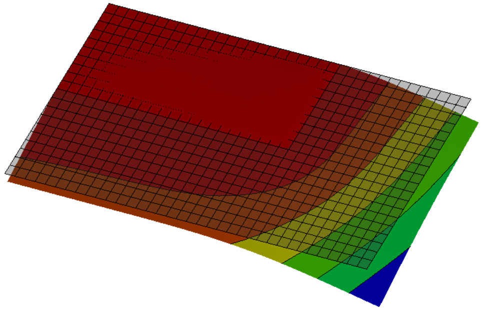

Figure 3: Displacement contours (elastic)

Whilst there are many results that we could contour, we have chosen to show only the maximum principal bending moment.

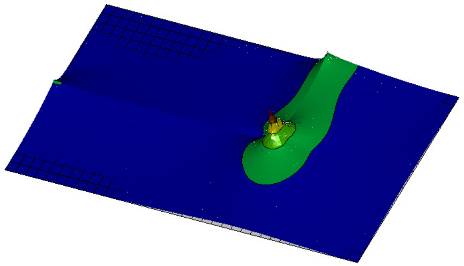

Figure 4: Maximum principal bending moment contours (elastic)

The contours of maximum principal bending moment of Figure 4 show, as expected, ridges over the internal supports and a peak value at the corner of the internal supports.

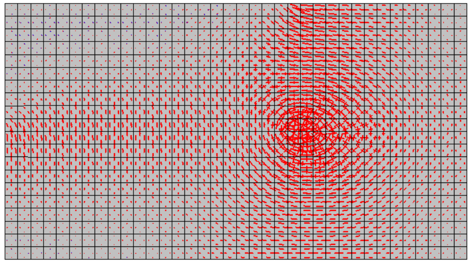

Figure 5: Principal bending vectors (elastic)

The principal moment vectors shown in Figure 5 provide more information on the distribution of moments. We use the convention of Red for Hogging and Blue for Sagging moments. The figure thus shows that the predominant moments are, as expected, hogging.

Limit Analysis Results for Left Hand Slab

Limit analysis attempts to identify the load at collapse. Collapse here is understood as collapse due to flexural (bending) failure. We use conventional yield line techniques which in terms of plasticity theory provide upper-bound or unsafe approximations to the collapse load. We also use equilibrium techniques for lower-bound or safe approximations to the collapse load. In this manner we are able to place bounds for the true collapse load for the slab.

The collapse load coming from limit analyses is expressed in terms of a load factor. The load factor is the factor that needs to be applied to the loading to cause collapse of the slab. The load factor is, obviously, dependent on both the assumed reinforcement and the applied load. We use the values previously defined for these quantities and present the resulting load factors. If other reinforcement or load is considered then the results may of course be scaled (providing the same patterns of reinforcement and load are used) such that the load factor is inversely proportional to the load and proportional to the assumed moment capacities.

A yield line analysis of the slab produced the result shown in Figure 6. The yield line pattern comprises a hogging line (red) across the slab coinciding with one of the lines of internal support. The load factor from this analysis is 1.48 implying that the slab can carry 1.48 times the applied load before collapse. Note, however, that the yield line technique is an upper bound approach and the true value may be less than this value.

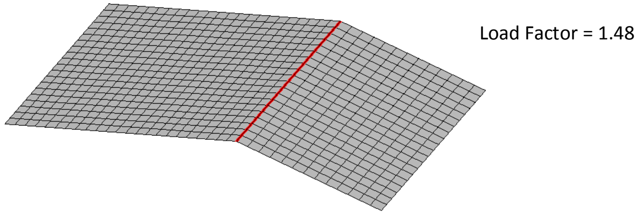

Figure 6: Yield line pattern and deflected shape (Top and bottom steel identical)

An equilibrium limit analysis of the slab using equal top and bottom steel provided a load factor of 1.45. As the yield line analysis and the equilibrium limit analysis provide results that bound the true solution then we can say that the true load factor lies between 1.45 and 1.48. For this particular example a tight bound has been found but in general we would advocate taking the lower of the two values for reasons of safety.

We present contours of maximum principal moment and principal moment vectors for the equilibrium limit solution in Figures 7 and 8.

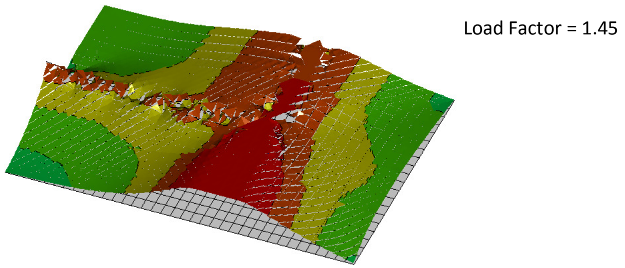

Figure 7: Maximum principal bending moment contours (equilibrium limit - Bottom = Top Steel)

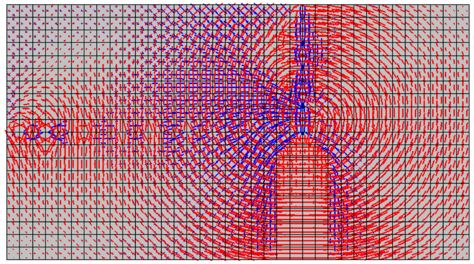

Figure 8: Principal moment vectors (equilibrium limit - Bottom = Top Steel)

Equilibrium limit analysis may be considered as a process of moment redistribution - a process of optimising a moment field so as to maximise load carrying capacity whilst not violating a given yield criterion – for the case of reinforced concrete the yield criterion is the Nielsen Biconic Yield Criterion. By comparing Figure 7 with Figure 4 one can see how, in this case the maximum principal moments are redistributed with the peak around the internal corner and ridges along the internal supports turning into flatter but wider distributions. Comparing Figure 8 with Figure 5 shows in further detail how the moment distribution changes with the limit solution invoking sagging moments (blue vectors) not present in the elastic solution.

Noting that for this problem the moment field is dominated by hogging moments, a further limit analysis was conducted with reduced bottom steel. For this analysis we reduced the bottom steel to 10% of the top steel. The yield line solution was exactly the same as for equal top and bottom steel. But the equilibrium limit analysis changed as shown in Figures 9 and 10.

Whilst there are changes evident in the maximum principal bending moment contours the biggest change is noted in the principal moment vectors where we see that the sagging vectors evident in Figure 8 have been eliminated. Contrary to intuition the load factor is slightly increased by reducing the bottom steel – we think we understand the reason for this but it does need further investigation.

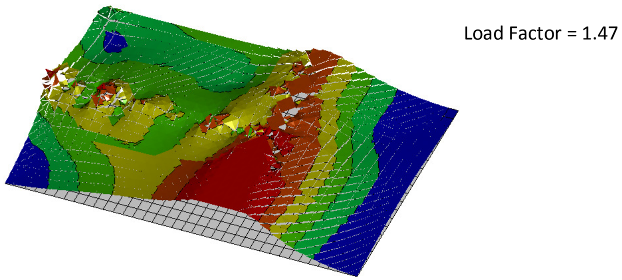

Figure 9: Maximum principal bending moment contours (equilibrium limit - Bottom = 0.1xTop Steel)

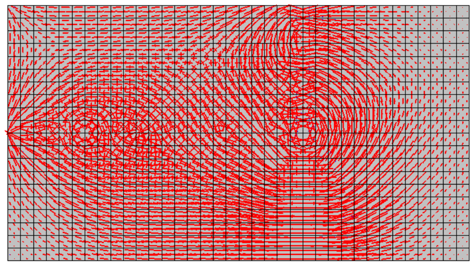

Figure 10: Principal moment vectors (equilibrium limit - Bottom = 0.1xTop Steel)

Discussion for Left Hand Slab

The analysis of this slab has produced a closely bounded solution giving load factor between 1.45 and 1.48. Noting that the moment field is dominated by hogging moments and analysis was conducted with a 90% reduction in bottom steel and with no significant change in the load carrying capacity of the slab this highlighted a way of economising on the steel used for the slab.

Geometry for Right Hand Slab

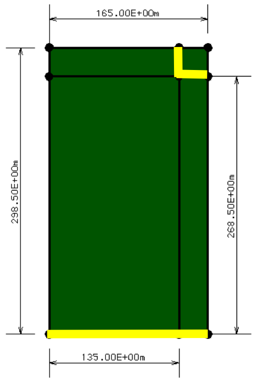

Dimensions in inches (not metres as suggested in figure)

Figure 11: Geometry and simple supports for roof slab

Properties for Right Hand Slab

The properties used for the elastic analysis were the same as those used for the left hand slab.

Although the slab has variable thickness, a uniform thickness of 10in was assumed for this work and a moment capacity of 10,000lb/in^2 – equal top and bottom steel.

Loads/Boundary Conditions for Right Hand Slab

The slab was assumed to be simply supported on the three lines shown in Figure 11. The slab was loaded with a uniform distributed load corresponding to the sum of a dead load and a live load. The dead load was based on an assumed density of concrete/steel composite over the given thickness whilst the live load was taken as a constant for the entire slab – the values used were the same as those for the left hand slab.

Elastic Analysis Results for Right Hand Slab

A mesh of 637 quadrilateral elements was used for the analyses. The elastic analysis used quadratic moment fields and the displaced shape is shown in Figure 12.

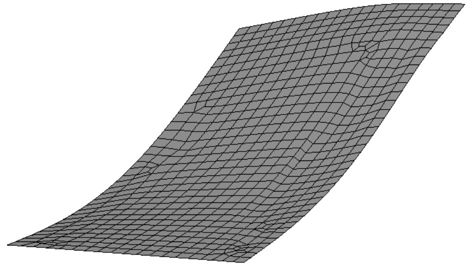

Figure 12: Displaced shape (elastic)

For the assumed elastic properties the maximum displacement was -0.31in towards the centre of the longest unsupported edge. A contour plot of displacement is shown in Figure 13. It is seen that the slab deflects upwards inside the column region and the maximum positive displacement is 0.02in at the free corner.

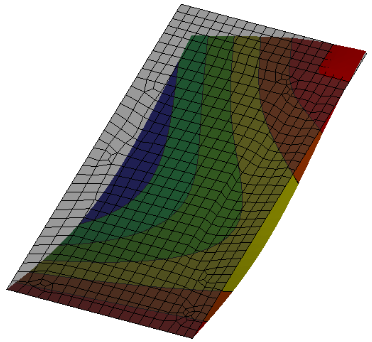

Figure 13: Displacement contours (elastic)

The principal bending moments are shown in Figure 14.

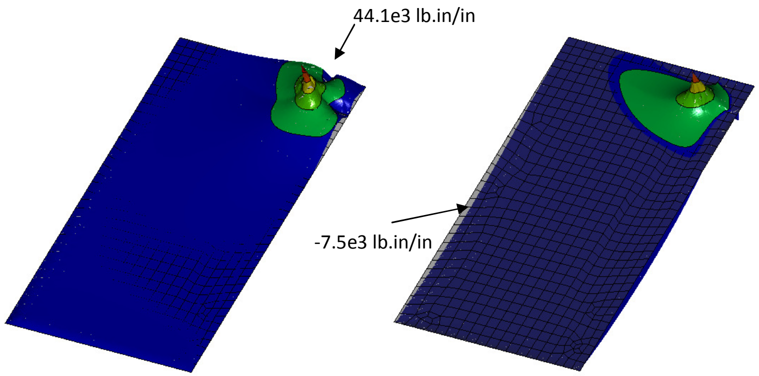

(a) Maximum principal moment (b) Minimum principal moment

Figure 14: Principal bending moment contours (elastic)

Both principal bending moments (maximum and minimum) peak, as expected, over the corner of the column. The maximum sagging moment appears towards the middle of the longest unsupported edge.

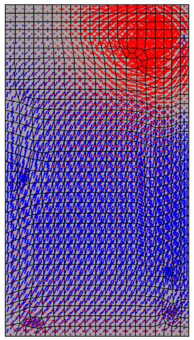

Figure 15: Principal bending vectors (elastic)

The principal moment vectors shown in Figure 15 provide more information on the distribution of moments. The figure shows a region of hogging around the column and a large sagging region between the column and wall support.

Limit Analysis Results for Right Hand Slab

We started this analysis with a regular mesh of 112 rectangular elements. The yield line analysis on this mesh produced the result shown in Figure 16. An equilibrium limit analysis on the same mesh produced a load factor of 1.15. The difference between the upper and lower bound load factors is quite large indicating that there is room for optimisation of the yield line pattern.

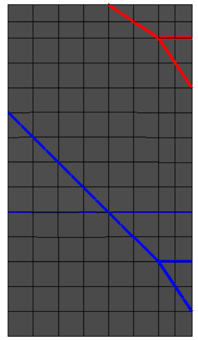

Load Factor = 1.47

Figure 16: Yield line pattern

A simplified mesh was constructed incorporating the collapse mechanism anticipated from the analysis of the regular mesh. By manually moving the four points defining the collapse mechanism the yield line load factor was brought down to 1.22 - almost 20% reduction in the predicted collapse load.

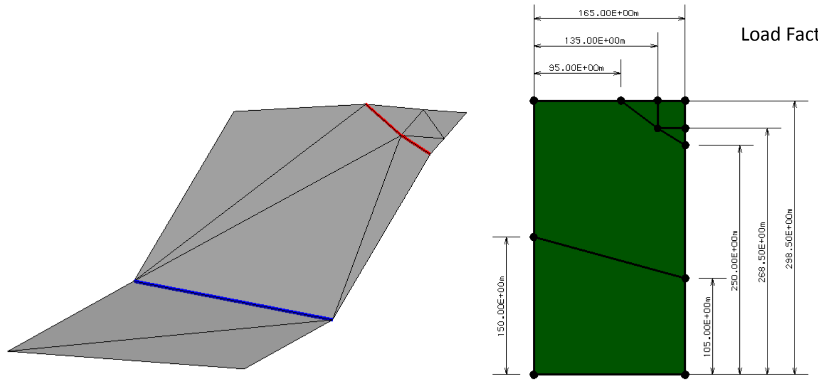

Load Factor = 1.22

Figure 17: Yield line pattern on deflected shape and optimal positions of points

An equilibrium limit analysis of the slab using equal top and bottom steel provided a load factor of 1.16. As the yield line analysis and the equilibrium limit analysis provide results that bound the true solution then we can say that the true load factor lies between 1.16 and 1.22. For this particular example a tight bound has been found but in general we would advocate taking the lower of the two values for reasons of safety.

We present contours of principal moment and principal moment vectors for the equilibrium limit solution in Figures 18 and 19.

Load Factor = 1.16

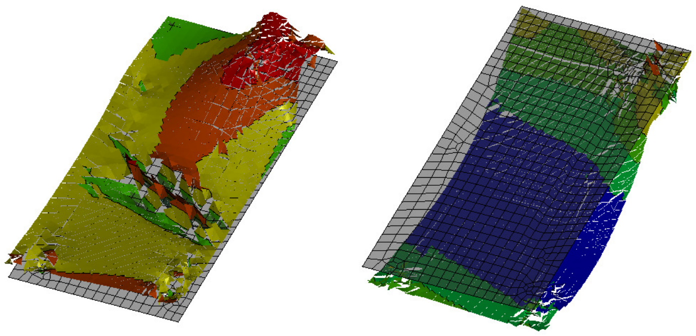

(a) Maximum principal moment (b) Minimum principal moment

Figure 18: Principal bending moment contours (equilibrium limit)

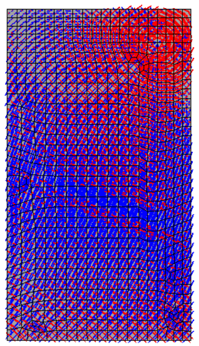

Figure 19: Principal moment vectors (equilibrium limit)

Comparing the elastic and equilibrium limit principal moments (Figures 14 & 18) shows that the effect of moment redistribution is to crop the elastic peak occurring around the corner of the column and concentrate the sagging moments in a diagonal band corresponding closely to the sagging yield line shown in Figure 17.

Discussion for Right Hand Slab

The analysis of this slab has produced a closely bounded solution giving load factor between 1.16 and 1.22. Unlike the left hand slab where the moment field was dominated by hogging moments, the right hand slab considered here has significant regions of both hogging and sagging moments. As such if single regular reinforcement mats are to be used for top and bottom steel there seems little sense in attempting to optimise the moment capacities. If, on the other hand, one were prepared to consider subdividing the slab

into regions of differing reinforcement, the moment vector plot of Figure 19 provides a useful indication of how one might perform this subdivision and what sort of reinforcement would be required in each region.

Closure

This document presents the results from elastic and limit analysis (both yield line and equilibrium limit) for a pair of reinforced concrete roof slabs. The two forms of limit analysis provide upper and lower bounds, respectively, for the collapse load of the slabs. In both cases tight bounds on the collapse load were obtained. For the right hand slab the initial mesh produced a significant (20%) overprediction of the true collapse load highlighting a potential defficiency in using the yield line technique for slab assessment – namely that the predicted collapse load is strongly dependent on the assumed collapse mechanism. Mesh refinement alone is not sufficient in yield line analysis as unless the mesh happens to place edges such that the true collapse mechanism can be formed, it produces an unsafe prediction of the collapse load. The lower bound technique (equilibrium limit analysis), on the other hand always provides a safe estimate of the collapse load irrespective of the mesh and quickly converges towards the true solution with mesh refinement.

Equilibrium Finite Elements

for safe structural analysis

and design optimisation